AIAA JOURNAL
Vol. 34, No. 4, April 1996

# Cable-Stiffened Pantographic Deployable Structures Part 1: Triangular Mast

Z. You* and S. Pellegrino†
*University of Cambridge, Cambridge CB2 1PZ, England, United Kingdom*

**A novel concept for a deployable mast is proposed. It is based on a three-dimensional pantograph with triangular cross section that is deployed and stiffened by two sets of cable elements: active and passive cable elements. Deployment is controlled by the active cables, whose overall length is controlled by an electric motor. After deployment, the stiffness of the mast is increased by pretensioning the passive cables. The layout of active and passive cables is such that all of them can be prestressed uniformly. The principle behind the selection of suitable cable layouts is presented in the paper. A small-scale, experimental model of the triangular mast has been built and tested. Its stiffness and deployment accuracy successfully demonstrate the potential of the new concept.**

## I. Introduction

THIS paper deals with one of the classic problems in deployable structures, how to make a deployable mast that is easy to design, inexpensive to make, and works well. A single solution, satisfying all of these general requirements, has yet to be found. Instead, several partial solutions have been identified, in the form of different structural concepts, such as telescopic masts, pantographs, coilable masts, STEMs, etc.[1–5] The particular solution relevant to this paper is the pantograph, whose simplest, two-dimensional form is the lazy tong, an assembly of straight rods of equal length connected by pivots in the middle and at the end. The pivot in the middle of each pair of rods is sometimes referred to as a scissor joint, because the pair of rods behaves in the same way as a pair of scissors.

Table 7.8 of Ref. 5 lists 20 different types of deployable masts, including two lazy-tong mechanisms and a triaxis pantograph, obtained by interconnecting three lazy tongs at angles of 60 deg, to form a triangular, articulated cross section. General design comments on these masts[5] are that they are good in terms of packaging and deployment control, but have low stiffness. Their performance can be improved by carefully designed latches, but joint nonlinearity is difficult to avoid and retraction would require complex delatching mechanisms. A lazy-tong mast with a length of 6 m but without any latches at the joints has been used on MAGSAT,[6] where the required structural stiffness was achieved by the use of graphite epoxy tubes for the members of the lazy tong. Similar masts had been used in previous missions.

This paper presents a radically different way of improving the performance of this type of deployable structure. The idea is that an extended, flexible pantograph can be transformed into a stiff lattice mast by means of a series of pretensioned cables. When the pantograph is folded these cables are slack, and hence the structure is still a single-degree-of-freedom mechanism that packages into a small volume. In the extended configuration, however, any required stiffness can be achieved by appropriately sizing the cross sections of the cables and of the members of the pantograph. Later papers in this series will show that the same approach has been successfully extended to pantographic ring structures, e.g., acting as edge beams of mesh reflectors, and will present a design optimization of this type of structures.

A cable-stiffened pantograph is built around a deployable backbone, i.e., the pantograph. It also contains a set of short passive cables that become taut when the pantograph is fully deployed and are pretensioned before any loads are applied to the mast. Finally, it contains a small number of active cables that control the deployment of the pantograph and the prestressing of the passive cables. Functionally, the passive cables replace the latching system required in previous concepts. The successful performance of a cable-stiffened pantographic structure requires that, after deployment, an overall state of prestress be set up, so that all cables are in a state of pretension. This way of using cables in deployment mechanisms is new, but there have been many successful applications of cables to control the deployment rate of spring-driven mechanisms, e.g., Ref. 5, to synchronize the deployment of telescopic booms[7] and also to deploy/retract, as well as to preload, the hinges of a rigid panel solar array.[8]

An alternative solution for increasing the fully deployed stiffness of a pantograph has been proposed by Zanardo.[9] This solution requires that, in addition to the planar lazy tongs that make up the required cross section of the mast, e.g., three interconnected lazy tongs to make a triangular mast, some shorter, hinged members be connected to the corner joints of the pantograph. These additional members are folded alongside the pantograph and become straight during deployment. This solution is compatible with the concept proposed in this series of papers, and it would be possible to replace some or all of the passive cables with hinged elements.

The concept of cable-stiffened pantographic masts was first proposed by Kwan and Pellegrino.[10,11] The original proposal was for a mast with a square cross section, deployed by two active cables. The flexural stiffness of this type of mast, however, varies considerably as the load direction changes, which is undesirable, and its active cables follow rather complicated routes. The more complete understanding of the concept of cable-stiffened pantographs that has been developed since the original proposal was made has afforded much greater freedom in the selection of suitable pantographs and routes for the active cables, as well as the layout of the passive cables. The triangular mast, shown in Fig. 1, is the end of product of this evolution.

The layout of this paper is as follows. Section II describes the geometry of the deployable backbone for the mast. Then, Sec. III discusses the way in which the active and passive cables are arranged, to control the deployment process and also to stiffen the fully deployed mast. A general technique for exploring a wide range of cable layouts has been developed, based on simple considerations of equilibrium for the basic building block of the mast. With this technique, it has been possible to find many different solutions that ensure a uniform state of pretension in all passive cables. Based on one of these solutions, a model mast has been built: its design and manufacture are presented in Sec. IV, together with a calculation of the motor torque required to deploy and prestress the model in a gravity environment. A range of stiffness and shape accuracy tests have been conducted on this model, and results from the testing program are presented and discussed in Sec. V. Section VI concludes the paper.

Received Dec. 5, 1994; revision received Sept. 24, 1995; accepted for publication Oct. 9, 1995. 

*Research Fellow, Department of Engineering, Trumpington Street. Student Member AIAA.

†Lecturer, Department of Engineering, Trumpington Street. Member AIAA.

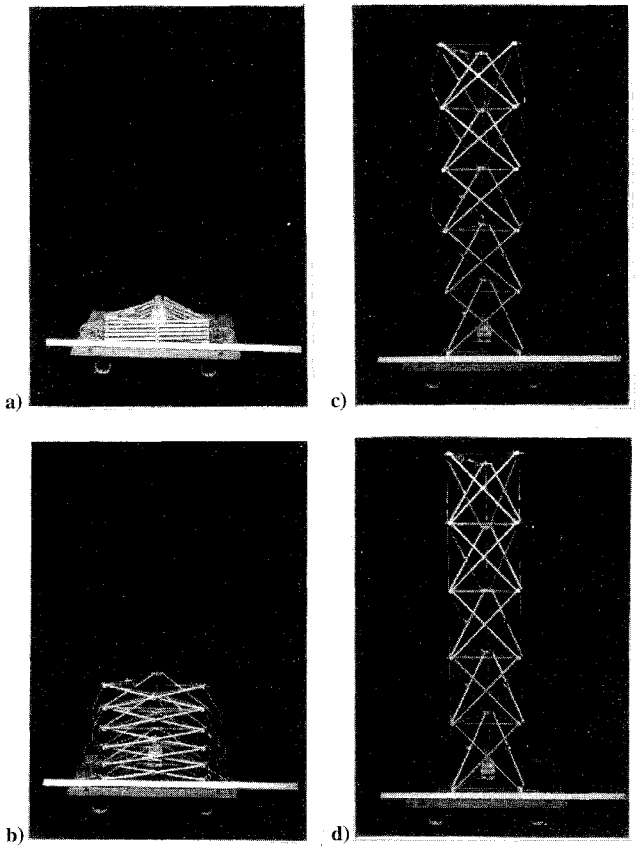


Fig. 1 Deployment sequence of 1.4-m mast.

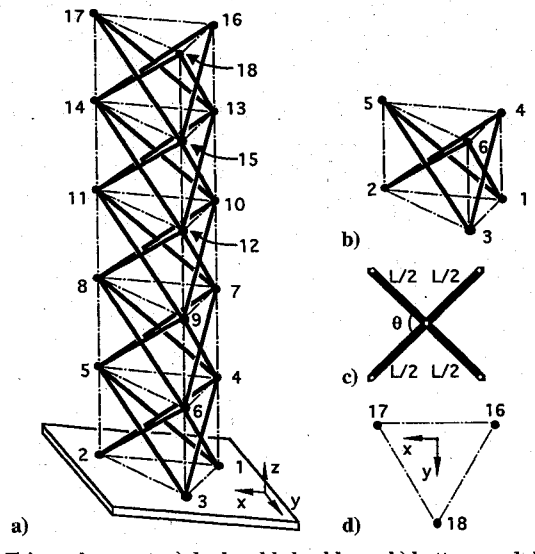


**Fig. 2 Triangular mast: a) deployable backbone, b) bottom module, c) pair of rods with connecting pin in the middle, and d) top view.**

## II. Deployable Backbone

The backbone of the triangular mast is shown in Fig. 2a. In this particular case, it consists of five identical triangular modules stacked on top of one another.

The basic module is shown in Fig. 2b. It consists of six rods forming three pairs; one such pair is shown in Fig. 2c. The three rod pairs forming the module lie on the side faces of a triangular prism and, in a top view of the module, form an equilateral triangle. A connection pin in the middle of each rod pair allows free rotation of the two rods: this motion is required to open and close the pantograph. The two joint assemblies connecting adjacent rod pairs that lie on different sides of the equilateral triangle also permit this rotation. No other motion of the rods is allowed. In the more formal language of kinematics, all direct rod–rod connections and also all rod–joint connections are revolute joints, with axes perpendicular to the sides of the equilateral triangle shown in Fig. 2d. This basic module can be folded and deployed freely: its configuration is defined by a single parameter $\theta$, defined in Fig. 2c, and hence the module is a single-degree-of-freedom mechanism.

The deployable backbone for the triangular mast is formed by stacking several modules on top of one another. In order for the modules to fit together, the parameter $\theta$ must have the same value for all modules, and so the entire pantograph has only one mechanism that allows it to change its shape continuously from nearly flat, i.e., fully folded ($\theta \cong 0$ deg), to an almost straight line, when the pantograph is fully extended ($\theta \cong 180$ deg). The next section explains how cables are used to activate this mechanism, and also to transform the pantograph into a stiff structure.

## III. Active and Passive Cables

During the deployment of the pantograph, the relative distances between the joints will vary. For instance, in Fig. 2a joints 4 and 5 will get closer during deployment, and joints 2 and 5 will get farther apart. Thus, active and passive cables can be used to deploy and stiffen the mast.[12] Active cables link joints that get closer during deployment. Shortening these cables will then cause the pantograph to deploy. Passive cables link joints that get farther apart during deployment. The passive cables have a constant length, approximately equal to the distance between these joints in the fully deployed configuration. These cables remain slack during deployment, but become taut in the fully deployed configuration, hence terminating deployment.

The active and passive cables have a farther important function. Once the structure is fully deployed, a small additional shortening of the active cables will subject all of the active and some or possibly all of the passive cables to a state of pretension. These cables will then become functional in a structural sense, thus stiffening the structure. It should be pointed out that there are many different ways of arranging the active and passive cables, and not all of these arrangements will allow all of the cables to be pretensioned.

The positions of the active and passive cables are chosen following some simple design rules. The number of active cables is kept as low as possible as these are rather complex elements. The positions of the passive cables are chosen to provide a high stiffness in the final shape: the interaction of the active and passive cables in setting up a uniform state of self-stress is also considered. Finally, ease of manufacture and operation are taken into account.

To understand how the backbone, the active cable, and the passive cables interact to form a state of self-stress, consider initially the one-module two-dimensional pantographic structure shown in Fig. 3, with two identical rods hinged in the middle. Excluding rigid-body motions the module has one degree of freedom, and so its configuration can be defined by the single parameter $\theta$. During deployment $\theta$ varies from $\theta_i$ (the initial deployment angle, which is close to zero) in the folded configuration to $\theta_f$ in the fully deployed configuration. Joints A and B and joints C and D get closer during deployment and may thus be connected by active cables whereas joints A and C and joints B and D get farther apart, and so can be connected by passive cables.

As this structure has only one mechanism, only one active cable would be enough to activate deployment and one passive cable enough to terminate deployment. Relying on the bending stiffness of the rods, however, is not an efficient way of making a stiff structure. To increase the stiffness of the fully deployed structure it is better to have many passive cables but, of course, it is necessary

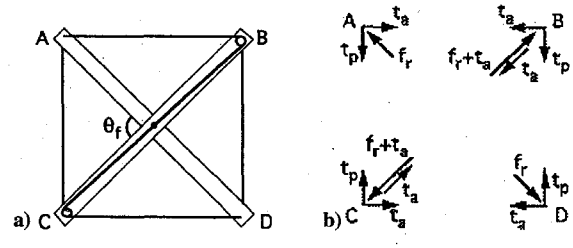


**Fig. 3a One-module, two-dimensional pantographic structure: a) backbone and cables and b) state of self-stress.**

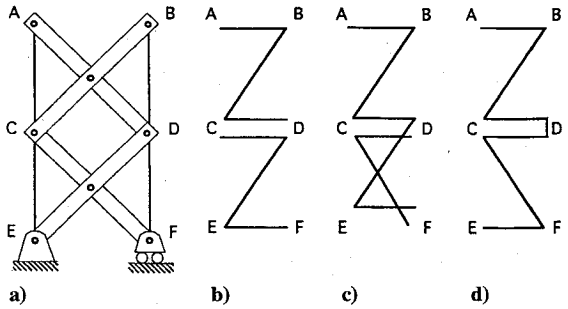


**Fig. 4 Two-module, two-dimensional pantographic structure: a) backbone and passive cables and b–d) different routes for active cables.**

to ensure that all cables can be prestressed when the structure is fully deployed. Kwan[4] has shown that the effective use of passive cables can significantly reduce the bending moments in the rods of a pantograph.

Therefore, consider using two passive cables and one active cable. The passive cables, each of length $L \sin(\theta_f/2)$, link joints A and C, and joints B and D. The active cable runs continuously from joints A to B to C to D. To have a pretension $t_p$ in the passive cables, vertical equilibrium of node A, see Fig. 3b, requires a compressive force $f_r$ in rod AD,

$$f_r = \frac{t_p}{\sin(\theta_f/2)} \tag{1}$$

Horizontal equilibrium of A then gives the tension $t_a$ in the active cable

$$t_a = t_p \cot(\theta_f/2) \tag{2}$$

Note that for an assembly with more than one module, if each module is in a state of self-stress, then the entire structure will also be in a state of self-stress. The preceding solution can easily be modified for these more complex structures. Consider, for example, the two-module structure shown in Fig. 4a. Four passive cables connect joints A to C, C to E, B to D, and D to F. Figures 4b–4d show three possible routes of the active cables. Figure 4b simply reproduces the one module solution for both top module ABCD and bottom module CDEF. Note that there are two active cables running from C to D providing a total tension of $2t_a$: this provides the tension $t_a$ needed for equilibrium of both the top and bottom modules. Figure 4c shows another possible arrangement that makes use of a long, continuous active cable. In this case a short additional cable provides the additional $t_a$ required to increase the total tension between C and D to $2t_a$. Figure 4d shows an arrangement that uses only one active cable. The tension $2t_a$ is now provided by a cable loop that runs twice between nodes C and D. Although these three active cables layouts are equivalent in terms of cable prestress, note that the compressive forces in the rods are different.

Consider now the active and passive cable design for a module of the triangular mast. Using the same approach as before, but now for the pantograph shown in Fig. 2b, three vertical passive cables, with lengths of $L \sin(\theta_f/2)$, are used. The active cable makes a complete loop of the top and bottom triangle: its complete route is through joints 1, 2, 3, 1, 6, 4, 5, and 6. The forces in the active cable and passive cables are related by

$$t_a = (t_p/2) \cot(\theta_f/2) \tag{3}$$

For a multimodule structure, there are many different routes of the active cables that provide the horizontal forces required to prestress the passive cables. Figure 5 shows three examples, involving one, two, or three active cables. In each of these solutions there are two active cable loops at the interface between two modules, to prestress both of them. However, there is a single loop at the very top and bottom of the structure. The cables are all firmly attached to a joint of the backbone at one end and wound onto a drum at the other end. They always run parallel to a rod when they go from one loop to the next. For practical reasons the inclined and horizontal cable segments that are joined are always in the plane of one pantograph;

**Table 1 Active cable routes for $n$-module mast**

| Route[a] | No. of active cables | No. of pulleys | Shortening of active cable, $d = L[\cos(\theta_i/2) - \cos(\theta_f/2)]$ |
|---|---|---|---|
| a | 1 | $7n$ | $6n \times d$ |
| b | 2 | $8n$ | $3n \times d$ |
| c | 3 | $9n - 3$ | $2n \times d$ |

[a]See Fig. 5.

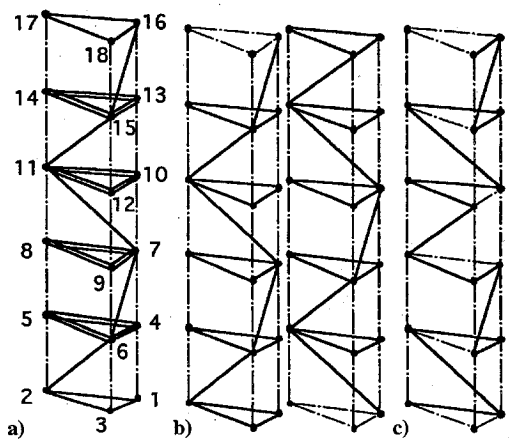


**Fig. 5 Active cable routes for a five-module mast: a) one active cable, b) two active cables, and c) three active cables (this solution has threefold rotational symmetry; hence the second and third cable routes are obtained by symmetry operations).**

this simplifies the positioning of the pulleys that support these cables. These arrangements are the three-dimensional counterpart to the active cables routes shown in Fig. 4 and require no less than two pulleys per joint. Table 1 shows a comparison of key parameters for the three arrangements of active cables, for an $n$-module mast. The most suitable design for a particular application can be selected by weighing all parameters in accord with practical demands.

The triangular mast is extended by shortening the active cables; the required shortening is given in the last column of Table 1. In the space environment, i.e., in the absence of gravity, deployment is resisted by friction at the pulleys and at the hinges. If friction is low, the forces in the active cables during deployment are fairly small. If two or more active cables are present, it is better to shorten all of them simultaneously so that no slackening of any active cables occurs, hence avoiding that a cable might come off a pulley. This can be achieved with a single deployment drum for all three sets of active cable routes shown in Fig. 5. Even the solutions shown in Figs. 5b and 5c, involving multiple cables, require that all cables change their lengths by the same amount, during deployment.

A theoretical problem with pantographs is that the active cable force required to expand them becomes infinite for an initial deployment angle $\theta_i = 0$, which means that active cables and rods are all in the same plane and, hence, they may become locked in an unstable equilibrium position. In practice, however, it is impossible to make $\theta_i = 0$, because of the physical size of joints and rods.

Finally, note that the triangular mast can be made automatically retractable either by adding a special passive cable connected, say, to the tip of the mast at one end and to a motorized drum at the other end, or by connecting the base joint assemblies to constant-force springs. This last solution has been tested in practice, as discussed in the next section.

## IV. Model Mast

A five-module triangular mast has been built and tested. The pantograph is made of Al-alloy tubes. The passive cables are made of Kevlar®, and the active cable is made of stainless steel. A turn buckle in each passive cable allows length adjustments up to 10 mm. The active cable follows the route in Fig. 5a. This solution, which requires a single active cable, has been chosen to reduce the complexity of the model. Full details on the components of the model mast are given in Table 2. When the model is fully deployed, it has

**Table 2 Components of model mast**

| Components | Rods | Passive cables | Active cable |
|---|---|---|---|
| Total no. | 30 | 15 | 1 |
| Density, kg/m$^3$ | 2700 | 1400 | 7830 |
| Young's modulus, N/mm$^2$ | 69 | 60 | 200 |
| Cross-sectional area, mm$^2$ | 24.640 (i.d. 3.86, o.d. 4.77 mm) | 0.292 | 0.220 |
| Length, mm | 400.0 | 282.8 | variable |

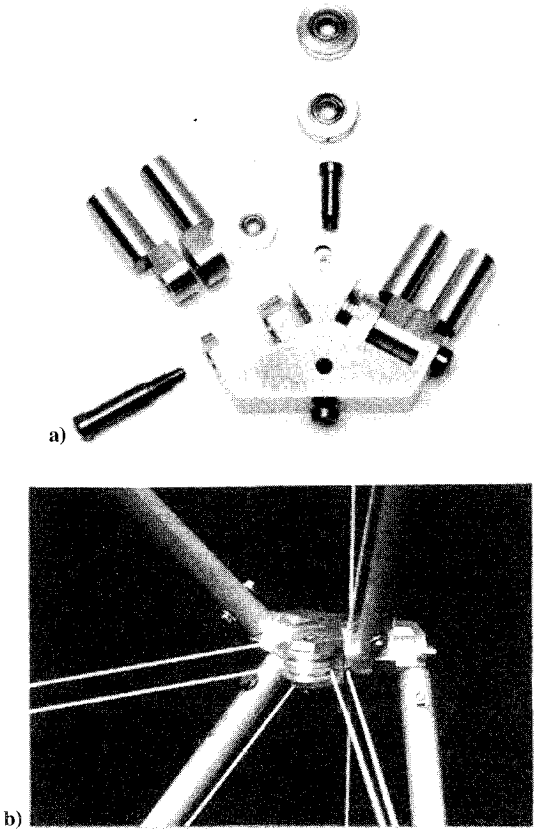


Fig. 6 Joint of model mast: a) component parts and b) assembled joint.

a deployment angle $\theta_f = 90$ deg and a height of 1.410 m; its height is reduced to 0.078 m in the fully folded configuration, see Fig. 1.

A joint assembly, Fig. 6, consists of a 12-mm-thick solid Al-alloy block that houses three 5-mm-diam steel pins. Two of the pins have axes lying in the midplane of the block. The rods of the pantograph and the vertical pulleys supporting the inclined segments of the active cable are connected to these pins. The third pin is perpendicular to the plane of the block; it holds the two horizontal pulleys that support the active cable loop. With this design the rods can open and close only in their own plane, but the angle between adjacent elements is kept constant at 60 deg. Provision is made for fixing the passive cables to the joint assembly. The horizontal pulleys have a diameter of 10 mm, whereas the vertical pulley has a diameter of 8 mm.

The model mast is mounted onto an Al-alloy plate with three radial slots at 120 deg, see Fig. 7. The three bottom joints run along these slots during deployment. At the center of the base plate there is a small dc motor with its gear box, driving a 80-mm-diam drum that winds in the active cable during deployment and pretensions the mast after deployment is completed.

To prevent the active cable from becoming slack during deployment, and also to retract the structure from its deployed state, three constant-force springs are connected to the three base joints. They apply outward forces of constant magnitude to these joints. Therefore, the mast will automatically fold itself if the active cable is

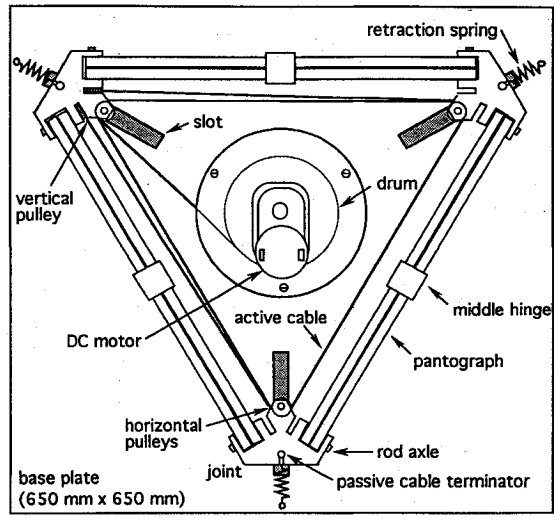


Fig. 7 Bottom module of model mast and its base plate, top view.

allowed to unwind from the drum. The retraction rate is controlled by the speed of release of the active cable, i.e., by the reverse rotation of the dc motor.

### A. Calculation of Motor Torque During Deployment

The maximum motor torque output required is estimated by considering the two different operating conditions of the motor: deployment and prestressing of the mast. In both cases, the motor torque is proportional to the active cable force $t_a$ and, hence, to estimate the motor torque it is necessary to estimate the maximum value of $t_a$. The calculation will be done using virtual work.[13]

Let us consider the slow deployment, in a gravity environment, of an $n$-module triangular mast whose rods have length $L$. Because inertia forces are negligibly small, the active cable force $t_a$ is in equilibrium with the retraction spring forces, the friction torques at the joints, and the weight of the mast (represented by concentrated forces at the joints). Whereas the magnitude of the first type of force is constant, the second and third types will vary according to the orientation of the mast with respect to gravity; they will be largest when the mast is deployed vertically up, and hence with gravity acting along the $-z$ direction (the coordinate system is defined in Fig. 2). Because the aim of this analysis is to estimate the maximum value of $t_a$, this is the only case that will be considered.

Consider the mast in a generic configuration, defined by the angle $\theta$. To calculate the value of $t_a$ required for static equilibrium in this configuration, a small configuration change of the mast, defined by the change $d\theta$ in the deployment angle, and the associated virtual work are considered.

Consider a pair of active cable forces acting on a pair of joints of the pantograph that are directly linked by a variable-length segment of active cable. The external work done by these forces is equal to the product of $t_a$ by the change of distance between the two joints, which is $L \sin(\theta/2)\,(d\theta/2)$. Because there are $6n$ such pairs of forces acting on the pantograph, and each pair does the same amount of work, the total virtual work done is

$$6t_a nL \sin(\theta/2)\,(d\theta/2) \tag{4}$$

The work done by a constant force spring connected to a base joint is equal to the magnitude of the force $f_s$ times the displacement of the base joint $(L/\sqrt{3})\sin(\theta/2)\,(d\theta/2)$. Hence, the total virtual work done by the three springs is

$$-\sqrt{3} f_s L \sin(\theta/2)\,(d\theta/2) \tag{5}$$

Next, the virtual work done by the weight $W$ of the mast is calculated. The $z$ components of the joint displacements are zero for the base joints 1, 2, and 3; they are $L\cos(\theta/2)\,(d\theta/2)$ for joints 4, 5, and 6, etc. Calculating the corresponding work contributions and adding them up gives

$$-W(n/2)L\cos(\theta/2)\,(d\theta/2) \tag{6}$$

Finally, the work done by the friction torques acting at the rod–joint hinges can be obtained simply by multiplying the total friction torque $T_f$ by the hinge rotation $d\theta/2$, where $T_f$ is the sum of the friction torques at all joints. This gives

$$-T_f\,(d\theta/2) \tag{7}$$

Friction in the pulleys supporting the active cable is negligible, because these pulleys are mounted on miniature ball bearings.

The total virtual work for the pantograph is obtained by adding up the four terms just obtained. The internal work is zero because the rods of the pantograph do not deform at all during the configuration change. The equation of virtual work is

$$6t_a nL\sin\frac{\theta}{2}\frac{d\theta}{2} - \sqrt{3}f_s L\sin\frac{\theta}{2}\frac{d\theta}{2} - W\frac{n}{2}L\cos\frac{\theta}{2}\frac{d\theta}{2} - T_f\frac{d\theta}{2} = 0 \tag{8}$$

Simplifying and rearranging Eq. (8) gives the following expression for $t_a$:

$$t_a = \frac{\sqrt{3}f_s}{6n} + \frac{W}{12}\cot\frac{\theta}{2} + \frac{T_f}{6nL\sin(\theta/2)} \tag{9}$$

Now, a preliminary estimate of the maximum active cable force required to deploy the model mast can be obtained from the first two terms on the right-hand side of Eq. (9), i.e., neglecting the effects of friction. The model has $n = 5$ modules, total weight $W = 20$ N, and retraction springs with constant tension $f_s = 18$ N. Since the first term in Eq. (9) is a constant, the maximum value of $t_a$ is reached when $\cot(\theta/2)$ is maximum, i.e., when $\theta$ is minimum. In the model, the minimum value of $\theta$ is $\theta_i = 3.4$ deg. Substituting these values into the first two terms of Eq. (9), while neglecting the third term, yields

$$t_a = 1.0 + 56.2 = 57.2 \text{ N}$$

To refine this estimate the value of $T_f$ is required. At a rod–joint connection, the friction torque is given by the resultant force in the rod that is approximately equal to the axial force in the rod $f_i$, multiplied by the friction coefficient $\mu$ and by the radius $r$ of the rod axle. The total friction torque is obtained by adding up the contributions from all of the axles and, because $\mu$ and $r$ are the same for all joints

$$T_f = \mu r\sum|f_i| \tag{10}$$

Note that each rod will appear twice in the summation and, since the axial force in a rod of a pantograph is usually discontinuous across the center connector, the two values of $f_i$ that correspond to the same rod will have different magnitudes.[14] To calculate $T_f$ according to Eq. (10) a full computer analysis of the mast is required (more to follow). However, a lower-bound estimate for $T_f$ can be obtained by virtual work, by noting that

$$\sum|f_i| \geq \left|\sum f_i\right| \tag{11}$$

Calculating the term on the left-hand side of Eq. (11) requires that the sign of the axial force carried by each bar of the pantograph be known, whereas the term $\sum f_i$ can be obtained from a global approach, as shown next. Note that Eq. (11) becomes an equality if the axial forces are all positive or all negative.

Virtual work can be used to calculate $\sum f_i$, from which the right-hand side of Eq. (11) can be obtained. The pantograph is in equilibrium, in a general configuration defined by the angle $\theta$, under its own weight $W$ and corresponding reaction forces from the base. Consider a virtual displacement of the mast, where each half-rod elongates by one unit and the base joints do not move at all. It can be shown by simple kinematics that the joint displacements compatible with these extensions are purely vertical and have magnitude $2/\sin(\theta/2)$ for joints 4, 5, and 6; $4/\sin(\theta/2)$ for joints 7, 8, and 9, etc. All displacements are directed upward. In this displacement system, each of the $n$ inclined segments of the active cable has to extend by two units.

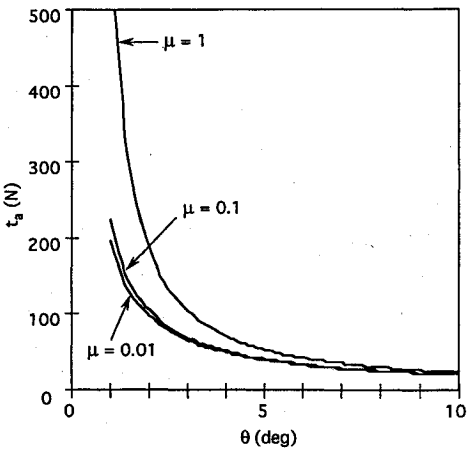


**Fig. 8 Variation of active cable tension during the initial deployment phase, for different values of the coefficient of friction.**

The external work is

$$-\frac{nW}{\sin(\theta/2)} \tag{12}$$

The internal work is

$$2nt_a + \sum f_i \tag{13}$$

Equating Eqs. (12) and (13) and solving for $\sum f_i$

$$\sum f_i = -2nt_a - \frac{nW}{\sin(\theta/2)} \tag{14}$$

This result can be used to estimate the total friction torque in any triangular mast and for any value of $\theta$. Equation (9) has been plotted in Fig. 8 using the given approximate expression for the third term, for three different values of $\mu$. It can be seen from the figure that $t_a$ decreases rapidly and becomes insensitive to the value of $\mu$ when $\theta > 5$ deg. This justifies the assumption that the third term in Eq. (9) can be neglected when making a preliminary estimate.

To refine the analysis for the specific case of interest, a computer analysis of the 5-module pantograph structure has been performed. The pantograph is in its initial configuration and is subject to concentrated forces at all joints (representing the weight $W$) and to spring forces $f_s$ at the base joints. The analysis shows that actually about half of the axial forces are tensile and half are compressive. Completing the calculation for a friction coefficient of, say, $\mu = 0.1$ and for an axle radius $r = 2.5$ mm, it is concluded that the maximum value of the active cable force, at the start of deployment, is

$$t_a \cong 61.3 \text{ N} \tag{15}$$

Note that the approximate estimate in Fig. 8, 60 N, was almost correct.

During deployment the value of $t_a$ decreases as $\theta$ increases, see Fig. 8. When the mast is nearly deployed ($\theta \cong 90$ deg) the minimum value of $t_a$, estimated from Eqs. (9), (10), and (14) according to the described procedure is $t_a \cong 3$ N.

### B. Calculation of Rotor Torque for Prestressing

Once deployment is complete the mast has to be prestressed to enable it to carry all operational loads without any cables going slack. Therefore, it is necessary to estimate the largest compressive axial force that will be induced in each cable by the various load conditions acting on the mast. In general, these load conditions will depend on the particular type of application. In this study, though, only three simple load cases are considered, three equal forces applied at the top three joints and acting in the $x$ direction (bending + torsion), in the $y$ direction (pure bending), and in the $z$ direction (axial). It is shown in Sec.V.A that the largest compressive passive cable force occurs for loads in the $y$ direction. Denoting by $P$ the resultant of these three forces, in a five-module mast the largest

compressive force in a passive cable is $-3.37P$, in the cable linking joints 3 and 6. This value has been obtained from a computer analysis of a linear-elastic pantograph with pin-jointed bars representing the passive cables. Further details on this kind of analysis are available elsewhere.[14,15] The total tension in cable 3-6, which must be positive, can be obtained by superposition of the initial prestress $t_p$ to the compressive force induced by the loading; hence,

$$t_p - 3.37P \geq 0 \tag{16}$$

The passive cable pretension $t_p$ is related to $t_a$ by Eq. (3) and, since $\theta_f = 90$ deg,

$$t_p = 2t_a \tag{17}$$

Substituting Eq. (17) into Eq. (16) gives

$$2t_a - 3.37P \geq 0 \tag{18}$$

from which

$$t_a \geq 1.68P \tag{19}$$

In the tests, the maximum $P$ is 11 N, and hence $t_a$ should be no less than 19 N to achieve sufficient prestress. Because an additional force of 3 N is required to resist the gravity loading and the constant-force springs, it can be concluded that the required value of the active cable force is at least

$$t_a \cong 22 \text{ N} \tag{20}$$

Comparing the requirements from the deployment and prestressing conditions, Eqs. (15) and (20), it is clear that the largest motor torque will be required to start deployment. The motor torque corresponding to $t_a = 61.3$ N and to a drum radius $R = 40$ mm is

$$t_a R = 61.3 \times 40 = 2452 \text{ Nmm} = 2.452 \text{ Nm} \tag{21}$$

Based on this estimate, the dc motor chosen was RS Part No. 320-607, with 130:1 gearbox reduction and with a maximum output speed of 20 rpm at 12 V. This motor has a peak torque of 4 Nm.

## V. Performance of Model Mast

Two types of tests have been conducted on the model:stiffness tests that are then compared with a computational model and accuracy tests to measure the variation in shape of the model mast after repeated deployments.

### A. Stiffness Tests

The behavior of the model mast was measured in three different configurations: 1) half-deployed, $\theta = 45$ deg; 2) fully deployed, $\theta = \theta_f = 90$ deg, without prestressing; and 3) fully deployed, $\theta = \theta_f = 90$ deg, with prestressing. A total load $P$ was applied at the top of the mast, one-third at each joint, first in the $y$ direction, then in the $z$ direction, and finally in the $x$ direction (the coordinate system is defined in Fig. 2). The linear-elastic response of the structure has been computed[15] and the results are plotted alongside the experimental results for comparison.

In the experiments, the force in the cables is measured by a tensometer. For a fixed gauge length, the lateral deflection of a cable because of a lateral force depends primarily on the tension in the cable and on the magnitude of the lateral force. According to this principle, a small spring steel strip is used to apply three concentrated forces on a cable and the bending moment is measured, by strain gauges, at a single section of the strip. The tension in the cable is related to this bending moment. The joint displacements are measured by means of a set of displacement transducers mounted on a rigid frame around the structure, specially installed for this measurement. The tip of each transducer is connected to the joint via a lightweight, straight tube so that the force applied on the structure by this connection is small enough to be neglected. All transducers are linked to a personal computer where the measured displacements are processed.

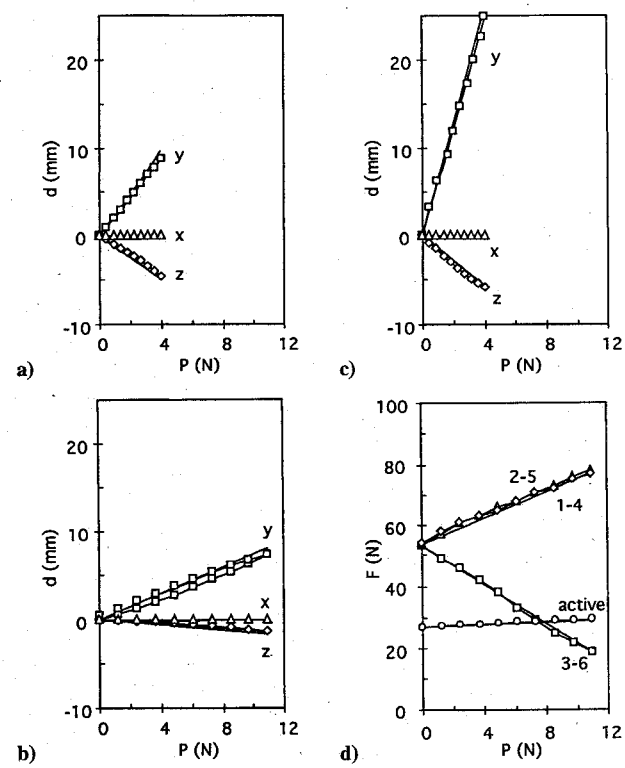


**Fig. 9 Response of model mast to a load $P$ in the $y$ direction; displacement components of joint 18 in a) configuration 1, b) configuration 2, c) configuration 3, and d) active and passive cable forces in configuration 3.**

The most interesting results are obtained when the mast is loaded in the $y$ direction, in pure bending. For this load case, Figs. 9a–9c show the displacements of joint 18 for the three configurations. Configurations 1 and 2 have been loaded to a lower level to avoid excessive displacements. In configuration 1 the stiffness is rather low. This is because the passive cables are slack, and hence the structure relies on the bending stiffness of the rods and their connecting hinges to bear loads. The same behavior is true in configuration 2, only now the stiffness is even lower. This is because the mast is now a longer and more slender structure, compare Figs. 1b and 1d. In configuration 3 the model mast has been prestressed: the active cable at 27 N and the passive cables at 53 N. This prestress level is higher than the minimum level, determined in Sec. IV.B. It can be seen from Fig. 9c that the mast is now much stiffer. The $y$ and $z$ displacements for $P = 4$ N are, respectively, only 8.8 and 6.6% of their values before prestressing.

Figure 9d shows the variation in prestress of the bottom three passive cables and the active cable during loading in the $y$ direction. As would be expected, the cable on the compression side of the structure reduces its tension, while the cables on the tension side increase theirs. The tension in the active cable changes very little during the test.

Figure 10a shows the variation in cable forces obtained for a compressive load $P$ in the $z$ direction, in configuration 3 and after prestressing the mast to the same level as before. It can be seen that the tension in the active cable increases, but the tensions in the passive cables decrease at a slower rate. Corresponding results for a load $P$ in the $x$ direction are shown in Fig. 10b. Comparing Figs. 9d and 10 it is found that the passive cable that will first lose its pretension is cable 3-6, see Fig. 9d, where a load of magnitude $P$ induces a change of tension $-3.37P$. The deflections for longitudinal loading ($-z$ direction) are much smaller than for transverse loading ($x$ direction) but vary linearly in both cases.

A general comparison of the experimental and computational results shows the mast to be a little stiffer than expected. This is because in the computational model joints of zero size are used instead of considering the physical size of joints, for the sake of simplicity. These idealized joints are located at the point where the passive

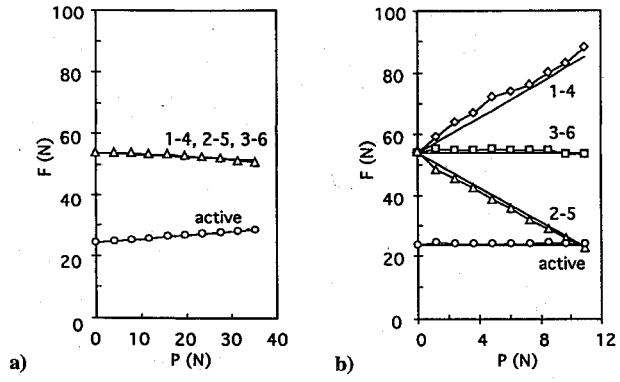


**Fig. 10 Active and passive cable forces; mast in configuration 3 and subject to a compressive load $P$ in a) the $z$ direction and b) the $x$ direction.**

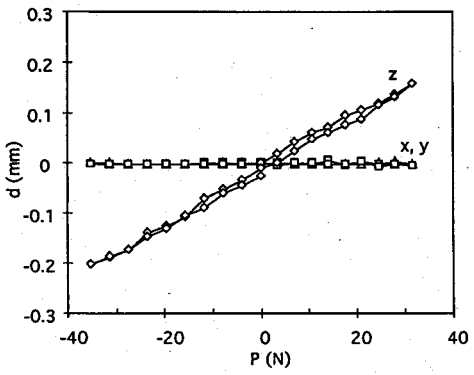


**Fig. 11 Displacement components of joint 18 during a complete loading and unloading cycle; mast in configuration 3; loads in $z$ direction.**

cables are terminated, and this simplification results in the computational model being slightly more slender than the actual structure.

Hysteresis can be seen in some of the loading–unloading paths, particularly in Fig. 9c, where a permanent deformation of about 0.5 mm has built up. This is because of the rather primitive method by which the passive cables have been connected to the joints and to the turnbuckles. The connections were made by knots fixed with glue. Slippage is unavoidable with this method; better methods of terminating cables have been used in later work, see the next paper in this series.

Load cycling has been explored further in Fig. 11 with loads in the positive and negative $z$ directions in succession. An interesting feature of Fig. 11 is the linearity of the loading path as it passes through zero. Prestressing the structure has removed any backlash that would be expected in simple latched structures.

### B. Deployment Tests

Shape accuracy has been tested by repeatedly folding and deploying the model mast, and then measuring the position of joints 16, 17, and 18. The joint coordinates were measured using a computerized Industrial Measurement System, based on three electronic theodolites.[16] This system has been developed to measure the three-dimensional coordinates of any target point within a triangular region whose vertices are defined by the theodolites. To take a measurement, all three theodolites are pointed toward the target point. Then, the horizontal and vertical angles measured by each theodolite are automatically sent to a personal computer and the coordinates of that point are calculated using a least-squares procedure, to achieve best accuracy. The system is initialized by measuring the distance between the end points of a 1-m ruler, at three different locations. This measurement system has an accuracy of 0.1 mm.

The model mast was deployed vertically up against gravity and horizontally in two different orientations. In each case, it was deployed 20 times. During each deployment test the active cable was wound in until a prestress level of 27 N was reached: automatic switch off of the deployment motor was triggered by a current limit, set in the power supply. The corresponding tension in the passive cables is then 53 N. The bottom three joints were fixed before any

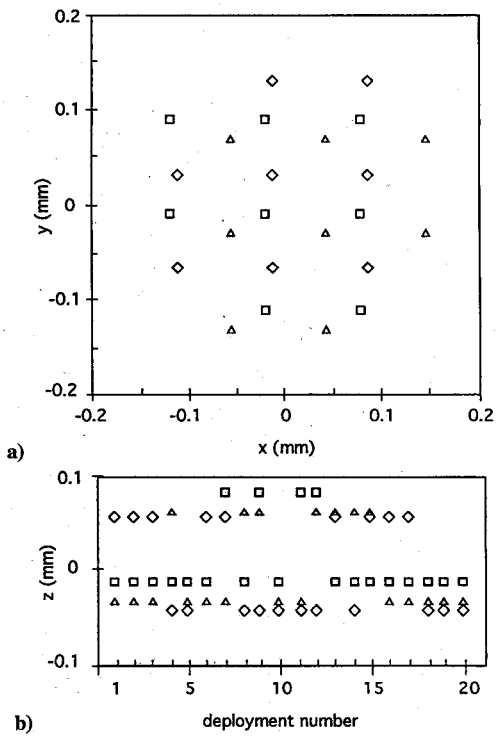


**Fig. 12 Position accuracy of joint 16 (□), joint 17 (◇), and joint 18 (△) for 20 fold-and-deploy cycles: a) $x$–$y$ components and b) $z$ components of position error.**

measurements took place. The positions of the top three and of some other joints were then measured before the mast was folded again.

Figure 12 shows the positions of joints 16, 17, and 18, both in the $z$ direction and in the $x$–$y$ plane, while deploying vertically up. The origin of both plots is the mean position for each joint. The results show a maximum deviation in the $z$ direction of 0.1 mm, and in the $x$–$y$ plane of 0.23 mm.

Other results, including distance errors between different pairs of joints of the mast, as well as the positions of joints for all three deployment orientations that are not shown here, are within the same range. In general, the maximum deviation of the top three joints is 0.1 mm in the direction of deployment, and 0.23 mm in the plane perpendicular to the direction of deployment.

## VI. Discussion

The triangular mast appears to provide a successful solution to all of the difficulties previously associated with pantographic deployable masts. In the past, one of the main areas of concern has been their poor shape accuracy and, in this respect, it is remarkable that the deployment accuracy of our relatively simple, proof-of-concept model should be as good as ±0.23 mm in the transverse direction, and ±0.1 mm in the longitudinal direction. Although this performance is rather good in absolute terms, we expect that it could be farther improved in a properly designed model. Therefore, we believe that the triangular mast would be a viable concept for applications requiring high-precision masts with lengths up to 10 m. Furthermore, the concept behind this mast lends itself to deployable structures with many other shapes, as will be shown in the next paper in this series.

Another area of concern associated with pantographic deployable structures is lack of stiffness. Here, it is important to note that the stiffness of the model mast toward the end of deployment, i.e., when the load-carrying structure is a pantograph, is only about 1/10 of the stiffness after prestressing. However, this is only an example of the kind of results that can be achieved by the proposed concept. The design of the model mast was not optimized; member properties were determined mainly by availability and cost. It can be expected that a better performance can be achieved by a suitably optimized design: this topic will be addressed in a later paper in this series.

One of the most important design constraints is buckling of the members of the pantograph, induced by the state of prestress, and

hence the cross-sectional area of the members of the pantograph tends to be much larger than that of the cables. Hence, the distortion of the mast during prestressing, produced by the uniform shortening of the members of the pantograph that are parallel to the active cable, is practically insignificant.

Finally, it is important to notice that the structural properties of the triangular mast depend crucially on the integrity of its active cables. Because there are many passive cables, there is a significant degree of redundancy, and hence the loss of a small number of passive cables would not be catastrophic. The number of active cables is small, however, and their reliability could become a major issue. If there is a single active cable, as in the model mast described in Sec. IV, this cable would be a single-failure point for the mast. There are two different ways of addressing this problem, either by using redundant cables, running along the same route and on the same set of pulleys, or by choosing one of the active cable arrangements that require two or more cables. If the first solution is chosen, failure of an active cable will not change appreciably the properties of the mast; if the second solution is chosen, failure of an active cable will lead to some loss of prestress and stiffness, but the mast will not be transformed into a mechanism.

## Acknowledgments

Z. You acknowledges with thanks financial support from the Cambridge Overseas Trust. This work was partially supported by a grant from the Engineering and Physical Sciences Research Council (Research Grant GR/F57113). We are grateful to C. R. Calladine, A. S. K. Kwan, and K. Miura for helpful comments during the course of this work, and to S. D. Guest for comments on an earlier version of this paper. We are also grateful to R. J. Denston for technical assistance.

## References

[1]Natori, M., and Miura, K., "Deployable Structures for Space Applications," AIAA Paper 85-0727, April 1985.

[2]Kitamura, T., Natori, M. C., Okazaki, K., and Yamashiro, K., "Developments of Extendible Beams for Space Applications," *Proceedings of the AIAA/AHS/ASEE Aerospace Design Conference* (Irvine, CA), AIAA, Washington, DC, 1993 (AIAA Paper 93-0977).

[3]Vieleers, A. M., and Preiswerk, P. R., "Extendible and Retractable Masts for Solar Array Deployments," *Proceedings of 3rd European Symposium Photovoltaic Generators in Space* (Bath, England, UK), European Space Agency, Noordwijk, The Netherlands, 1982, pp. 201–207 (ESA-SP-173).

[4]Kwan, A. S. K., "A Pantographic Deployable Mast," Ph.D. Thesis, Cambridge Univ., Cambridge, England, UK, Feb. 1991.

[5]Rauschenbach, H. S., *Solar Cell Array Design Handbook (The Principles and Technology of Photovoltaic Energy Conversion)*, Van Nostrand Reinhold, New York, 1980.

[6]Smola, J. F., Radford, W. E., and Reitz, M. H., "The Magsat Magnetometer Boom," *Proceedings of the 14th Aerospace Mechanisms Symposium*, NASA-CP-2127, 1980, pp. 267–278.

[7]Becchi, P., and Dell'Amico, S., "Design and Testing of a Deployable, Retrievable Boom for Space Applications," *Proceedings of 23rd Aerospace Mechanisms Symposium*, NASA-CP-3032, 1989, pp. 101–112.

[8]De Kam, J., "EURECA Application of the RARA Solar Array," *Proceedings of 5th European Symposium Photovoltaic Generators in Space* (Scheveningen, The Netherlands), European Space Agency, 1986, pp. 105–114 (ESA-SP-267).

[9]Zanardo, A., "Considerazioni su di un braccio estensibile per l'impiego nello spazio," Istituto di Meccanica Applicata alle Macchine, Rept. 87, Univ. of Padua, Padua, Italy, 1984.

[10]Kwan, A. S. K., and Pellegrino, S., "A Cable-Rigidised 3D Pantograph," *Proceedings of 4th European Space Mechanisms and Tribology Symposium* (Cannes, France), European Space Agency, 1990, pp. 149–154 (ESA-SP-299).

[11]Kwan, A. S. K., and Pellegrino, S., "The Pantographic Deployable Mast: Design, Structural Performance and Deployment Tests," *Rapidly Assembled Structures*, edited by P. S. Bulson, Computational Mechanics, Southampton, England, UK, 1991, pp. 213–224.

[12]Kwan, A. S. K., You, Z., and Pellegrino, S., "Active and Passive Cable Elements in Deployable Masts," *International Journal of Space Structures*, Vol. 8, Nos. 1, 2, 1993, pp. 29–40.

[13]Neal, B. G., *Structural Theorems and Their Applications*, Pergamon, Oxford, England, UK, 1964.

[14]Kwan, A. S. K., and Pellegrino, S., "Matrix Formulation of Macro-Elements for Deployable Structures," *Computers and Structures*, Vol. 50, No. 2, 1994, pp. 237–254.

[15]You, Z., "Deployable Structures for Mesh and Reflector Antennas," Ph.D. Dissertation, Cambridge Univ., Cambridge, England, UK, Aug. 1994.

[16]Kwan, A. S. K., and You, Z., "User Guide to Theo3, an Industrial Measurement System Using Three Zeiss ETh2 Theodolites," Engineering Dept., Cambridge Univ., CUED/D-STRUCT/TR142, Cambridge, England, UK, 1993.